

Electroresponsive Alginate-Based Hydrogel for Controlled Release of Hydrophobic Drugs

**Anna Puiggali-Jou,^{a,b,*} Eric Cazorla,^a Guillem Ruano,^a Ismael Babeli,^a
Maria-Pau Ginebra,^{b,c,d} Jose García-Torres^{b,c,*} and Carlos Alemán^{a,b,*}**

^a *Departament d'Enginyeria Química, EEBE, Universitat Politècnica de Catalunya, C/
Eduard Maristany, 10-14, 08019, Barcelona, Spain*

^b *Barcelona Research Center in Multiscale Science and Engineering, Universitat
Politècnica de Catalunya, 08930 Barcelona, Spain*

^c *Biomaterials, Biomechanics and Tissue Engineering Group, Departament de Ciència i
Enginyeria de Materials, Universitat Politècnica de Catalunya (UPC), 08930
Barcelona, Spain*

* anna.puiggali@upc.edu,

jose.manuel.garcia-torres@upc.edu and carlos.aleman@upc.edu

ABSTRACT

Stimuli-responsive biomaterials have attracted significant attention for the construction of on-demand drug release systems. The possibility of using external stimulation to trigger drug release is particularly enticing for hydrophobic compounds, which are not easily released by simple diffusion. In this work, an electrochemically active hydrogel, which has been prepared by gelling a mixture of poly(3,4-ethylenedioxythiophene): polystyrene sulfonate (PEDOT:PSS) and alginate (Alg), has been loaded with curcumin (CUR), a hydrophobic drug with a wide spectrum of clinical applications. The PEDOT/Alg hydrogel is electrochemically active and organizes as segregated PEDOT- and Alg-rich domains, explaining its behaviour as an electroresponsive drug delivery system. When loaded with CUR, the hydrogel demonstrates a controlled drug release upon application of a negative electrical voltage. Comparison with the release profiles obtained applying a positive voltage and in absence of electrical stimuli, indicates that the release mechanism dominating this system is complex due not only to the intermolecular interactions between the drug and the polymeric network but also to the loading of a hydrophobic drug in a water-containing delivery system.

INTRODUCTION

Intrinsically conducting polymers (CPs) have gained much attention as materials capable of stimuli-responsive drug delivery.¹⁻⁶ Among CPs, poly(3,4-ethylenedioxythiophene) (PEDOT) has evolved as a highly promising platform for delivering therapeutic agents, as it has excellent electroactive properties, stability, biocompatibility and is relatively simple to prepare.⁷⁻¹² Tunable drug release from PEDOT is based on electrically driven alterations in redox state, causing subsequent changes in polymer properties (*e.g.* changes in volume and hydrophilic/hydrophobic balance).¹³ Moreover, PEDOT has been used for drug delivery from carriers in different formats, for example, PEDOT nanoparticles,^{14,15} fibers,¹⁶⁻¹⁸ films,¹⁹⁻²² and hydrogels.²³⁻²⁵

Hydrogels-based delivery systems can leverage therapeutic beneficial outcomes and have found clinical use. This is because hydrogels not only can provide spatial and temporal control over the release of small molecules and macromolecular drugs,²⁶⁻³³ but also, exhibit tunable physical properties, controllable degradability, the capability to protect labile drugs from degradation and responsiveness to external stimuli. Therefore, hydrogels can serve as potential drug delivery platforms in which the release of loaded drugs is controlled by physicochemical interactions that can be easily modified by physical parameters (*e.g.* voltage, light, and temperature). Despite such interesting properties, the amount of drug release studies involving PEDOT-based hydrogels is very scarce.^{23-25,33} Kleber *et al.*²³ studied the release of fluorescein and dexamethasone from iridium oxide electrodes coated by a conducting hydrogel that was obtained by photocrosslinking poly(dimethylacrylamide-*co*-4-methacryloyloxy benzophenone-*co*-4-styrenesulfonate) and, subsequently, electropolymerizing PEDOT through the hydrogel network. Molina *et al.*²⁴ regulated the release of vitamin K3 from a semi-interpenetrated hydrogel prepared by electropolymerizing a hydrophilic PEDOT derivative within a poly-

γ -glutamic acid biohydrogel containing PEDOT nanoparticles. Zhang and co-workers²⁵ formed hydrogels by mixing a β -cyclodextrin polymer solution with a dispersion of PEDOT, which was obtained by oxidative polymerization in the presence of adamantyl-modified sulfate alginate. This matrix was used to encapsulate and to proliferate myoblast cells, which were released by adding the β -cyclodextrin monomer. On the other hand, Chikar *et al.*³³ formed a dual coating system by depositing an RGD-functionalized alginate hydrogel on an electrode previously coated with PEDOT. Interestingly, a trophic factor loaded inside the hydrogel was released by electrostimulating the coated electrode.

In this study, a new PEDOT-based electroactive hydrogel is explored as a carrier platform for electrically triggered drug delivery. The hydrogel is easily prepared by mixing polystyrenesulfonate-doped PEDOT (PEDOT:PSS), a biocompatible CP widely used for bioelectronics and tissue engineering,³⁴⁻³⁷ and alginic acid (AA) aqueous solution. Although alginate-based hydrogels are extensively used in biomedicine,³⁸⁻⁴⁰ the incorporation of CP confers electric-field responsive properties to the resulting material, hereafter named PEDOT/Alg-h. Drug delivery assays have been conducted using curcumin (CUR), a hydrophobic compound with a wide spectrum of biological and pharmacological activity, such as antioxidant, anti-inflammatory, antimicrobial, anticarcinogenic, hepatic- and nephroprotective, and hypoglycemic effects, among others.⁴¹⁻⁴⁵ The release of *in situ* loaded CUR is controlled by applying a potential of – 1.0 V to the hydrogel. Due to the advantages associated with the simplicity of the synthetic and loading processes, the outstanding properties of the hydrogel, and its response to the electric field for the dosage-controlled release of a drug, PEDOT/Alg-h should be considered as a promising carrier for on-demand release of bioactive substances.

RESULTS AND DISCUSSION

Preparation of unloaded and drug-loaded hydrogels

The process used to prepare PEDOT/Alg-h is sketched in Figure 1a. More specifically, equal volumes (20 mL) of a 1.3 wt.% PEDOT:PSS aqueous dispersion and an 8 wt.% alginic acid (AA) water:ethanol (4:1 v/v) solution were mixed at room temperature with vigorous stirring for 20 min. To prepare hydrogel films with a controlled, reproducible and homogeneous thickness, an indium tin oxide (ITO) coated polyethylene terephthalate (PET) sheet (4 cm × 2 cm × 0.01 cm) was sandwiched between two cover glasses separated 1 mm by plastic strips, which allowed creating a cavity with a defined volume. Then, a fixed volume of the PEDOT:PSS + AA mixture (0.7 mL) was introduced in the cavity to get films with reproducible thicknesses (see Figure 1). Finally, the previous assembly was immersed in a petri dish containing a 10 wt.% CaCl₂ aqueous solution to gel the mixture and obtain the hydrogel. The assembly was kept in the CaCl₂ solution for at least 24 h to assure complete gelation. The excess of AA and the leaving PSS chains (*i.e.* those replaced by Alg) were removed from the hydrogel by thoroughly washing it with abundant water. After disassembling, the hydrogels remained onto the ITO-coated PET sheet for the electrochemical studies.

CUR-loaded PEDOT/Alg-h samples, hereafter named PEDOT/Alg(CUR)-h, were obtained by applying the previous procedure but using a CUR ethanol solution (5 mg/mL) for preparing the 8 wt.% AA water:ethanol (4:1 v/v) solution. Besides, CUR-loaded and unloaded alginate hydrogels, hereafter abbreviated Alg(CUR)-h and Alg-h, respectively, were used as controls. Alg(CUR)-h was obtained by gelling with CaCl₂ (10 wt.%; 24 h) a 4 wt.% AA water:ethanol (9:1 v/v) solution, which was prepared again using the CUR ethanol solution. Alg-h was attained using the same procedure detailed above but without

including CUR in the ethanol used to prepare the AA solution. After the crosslinking, the concentration of CUR loaded in both PEDOT/Alg(CUR)-h and Alg(CUR)-h was 0.492 ± 0.005 and 0.474 ± 0.006 mg/mL, respectively. A complete description of the procedures used to prepare PEDOT/Alg-h, PEDOT/Alg(CUR)-h, Alg-h, and Alg(CUR)-h, which are shown in Figure 1b, is provided in the Supporting Information. The dark blue color of PEDOT/Alg-h and PEDOT/Alg(CUR)-h corresponds to the color of PEDOT:PSS, which dominates over those of Alg and CUR. Instead, translucent Alg-h samples become opaque and orange when CUR loads.

All hydrogels were initially characterized by FTIR spectroscopy. Structural fingerprints of all the components in the hydrogel were identified in the spectra (Figure 1c). Thus, all spectra show the following absorption bands characteristic of alginate hydrogels: (1) asymmetric and symmetric C=O stretching (1597 and 1413 cm^{-1} , respectively), C–O–C stretching (1028 cm^{-1}) and O–H stretching (broad band at ~ 3300 cm^{-1}).⁴⁶ In contrast, PEDOT-containing hydrogels show additional bands at 1289 and 1127 cm^{-1} (vibrations of the fused dioxane ring) and 761 cm^{-1} (stretch of the C–S bond). Moreover, the band at 1162 cm^{-1} has been associated with the S–O vibrations of residual PSS chains (*i.e.* those that were not substituted by the Alg chains). Finally, even though some of the characteristic bands of CUR overlap with those of PEDOT and specially those of alginate, CUR presence is also detected in the FTIR spectra of PEDOT/Alg(CUR)-h and Alg(CUR)-h. The peaks at 1522 and 756 cm^{-1} can be attributed to the C=O stretching and *cis*-CH vibration of CUR, which proves the incorporation of the drug in PEDOT/Alg(CUR)-h and Alg(CUR)-h.

The swelling ratio (SR), which expresses the ability to absorb water, was very high for all evaluated hydrogels (Figure 1d). The SR for Alg-h and PEDOT/Alg-h were similar (*i.e.* $1207\% \pm 21\%$ and $1240\% \pm 35\%$, respectively) suggesting that the crosslinking

density is comparable for both systems. According to the classical “egg-box” model, chain-chain associations in Alg-h occur by the ionic binding of each divalent Ca^{2+} ion with two alginate chains through the corresponding guluronate blocks.⁴⁷ Apparently, this binding model does not undergo major alterations by oxidized PEDOT chains, which are positively charged, and can compete with Ca^{2+} ions for interacting with Alg chains. On the other hand, the SR is higher for Alg(CUR)-h and PEDOT/Alg(CUR)-h than for unloaded hydrogels (*i.e.* SR increases 9% and 7% in comparison to Alg-h and PEDOT/Alg-h, respectively). This observation suggests that the drug has some adverse effect on the crosslinked structures of the hydrogels, slightly reducing the density of crosslinks and, therefore, increasing the free volume. Thus, the CUR would preferentially interact with Ca^{2+} ions and PEDOT chains, reducing their ability to bind Alg chains and, consequently, the crosslinking density concerning unloaded hydrogels.

Cytotoxicity

Since the final application of the developed material is its therapeutic utilization as a drug carrier, it is essential to study the biocompatibility of the employed material itself (*i.e.* without the drug). For this purpose, *in vitro* cell adhesion and cell proliferation studies were performed by MTT assays on Alg-h and PEDOT/Alg-h, which served as substrates for fibroblasts derived from normal skin (Hff) and osteosarcoma (MG-63) cells.

Figure 2 displays cell viabilities after 24 h (cell adhesion) and 7 days (cell proliferation) for the hydrogels and the tissue culture polystyrene (TCPS) used as a control substrate. These results reveal a clear dependence of the proliferation rate on cell type. It is well-known that cell tissues present different mechanical properties and this may affect cell behavior.⁴⁸⁻⁵¹ As expected, cells had a similar adhesion to both systems

without exhibiting a reduction in cell viability (Figure 2a). After 7 days (Figure 2b), Hff cells exhibited a higher affinity towards both Alg-h and PEDOT/Alg-h than MG-63 cells. This has been attributed to the stiffness of the material. Alg-based hydrogels without additional either covalent crosslinking or inorganic fillers are too low in stiffness to promote proliferation and spreading of hard tissue cells like bone. This hypothesis is strongly supported by previous microindentation results, which showed that the elastic modulus of the dermis is ~ 35 kPa⁵² while that for bone is in the 10.4–20.7 GPa range.⁵³ Therefore, PEDOT/Alg-h would be more suitable to be used in soft tissues like skin, nervous system, adipose, and cardiac tissues.

Morphology of unloaded and drug-loaded hydrogels

High and low magnification SEM micrographs of the cross-section and surface of the loaded and unloaded hydrogels are displayed in Figure 3a. As can be observed, the cross-sections of all hydrogels are qualitatively the same and they are characterized by showing an open and interconnected porous structure. The cross-section porosity is higher for PEDOT/Alg-h, PEDOT/Alg(CUR)-h, and Alg(CUR)-h than for Alg-h, which is consistent with the higher electrochemical activity of the formers (see below). However, different pore sizes and pore areas are measured for the different hydrogels as shown in the histograms in Figures 3b-c. The average diameters of the cross-sectional pores increase as follows: Alg-h (0.9 ± 0.3 μm) < Alg(CUR)-h (1.9 ± 0.6 μm) < PEDOT/Alg-h (2.0 ± 1.0 μm) < PEDOT/Alg(CUR)-h (2.6 ± 0.8 μm). Obviously, the area of the pores follows the same trend Alg-h (0.9 ± 0.6 μm^2) < Alg(CUR)-h (2.8 ± 1.6 μm^2) < PEDOT/Alg-h (3.2 ± 1.5 μm^2) < PEDOT/Alg(CUR)-h (4.6 ± 2.5 μm^2). These results suggest that the presence of either CUR or PEDOT in the hydrogel could increase the distance between alginate chains, explaining the presence of bigger pores compared to

the bare alginate hydrogel. No significant differences are observed between Alg(CUR)-h and PEDOT/Alg-h. However, the simultaneous presence of CUR and PEDOT within the hydrogel results in a new increase in pore size and pore area meaning that a new reduction in the cross-linking takes place. On the other hand, the surface morphology presents no pores and a smooth appearance. Besides, the superficial and cross-sectional morphology of the CUR-loaded hydrogels is very similar to that of the unloaded ones, suggesting that the drug is homogeneously distributed.

TEM images of the stained PEDOT/Alg-h are shown in Figure 4a. Dark regions correspond to the anionic sites of Alg that were selectively stained with 1% uranyl acetate (UAc), while bright grey regions correspond to PEDOT. Although contrast regions associated with Alg-rich domains present a continuous structure, which explains the mechanical integrity of the hydrogel, bright regions can be distinguished. In some cases, the latter PEDOT-rich domains appear as interconnected nanometric grey spots embedded inside Alg-rich domains, while in other cases PEDOT-rich domains appear as micrometric ($\sim 1 \mu\text{m}$) corpuscles interrupting the Alg-rich regions. The identification Alg-rich domains, in which PEDOT chains coexist with the predominant Alg chains, as well as of PEDOT-rich domains with the opposite organization, fully support the influence of the CP on the cross-linking between Alg chains. This partially segregated structure is also clearly reflected in TEM micrographs of unstained samples (Figure 4b), in which dark regions correspond to PEDOT-rich domains due to the remarkable electron scattering properties of the CP. The microstructure showed by both stained and unstained samples of PEDOT/Alg-h with both components coexisting in many regions has an impact on electroactivity, as shown below.

Electrochemical characterization

Unloaded and CUR-loaded PEDOT/Alg-h and Alg-h were characterized by cyclic voltammetry (CV) and galvanostatic charge-discharge (GCD) using a CaCl₂ 5 wt.% aqueous solution as supporting electrolyte. Figure 5a shows the control cyclic voltammograms recorded for the different hydrogels. As can be observed, all the voltammograms are qualitatively the same: quasi-rectangular and symmetric in shape without redox peaks which are attributed to the reversibility of the non-faradaic adsorption/desorption process of Ca²⁺ ions onto the hydrogel surface during the potential scan. Thus, both the Alg-rich phases of PEDOT/Alg-h and Alg-h are considered ionically conductive since Alg chains are negatively charged and the formed hydrogels contain an aqueous electrolyte inside (*i.e.* CaCl₂ dissolved in water). Comparison of the unloaded hydrogels indicates that the electrochemical activity is slightly higher for PEDOT/Alg-h than for Alg-h which can be attributed to the electronic contribution of PEDOT but also the higher SR both making the Ca²⁺ adsorption/desorption process more efficient.

CUR-loaded hydrogels display an increment in the area of the voltammograms compared to the unloaded ones, which is very significant for Alg(CUR)-h. The higher electrochemical activity of Alg(CUR)-h indicates that the diffusion and migration of ions during the potential scan experienced a drastic increase, which is fully consistent with the high SR value obtained for the Alg(CUR)-h. Thus, the increment in the voltammetric area of Alg(CUR)-h with respect to Alg-h suggests that CUR preferentially interacts with Ca²⁺, reducing the crosslinking density and facilitating the ion diffusion with respect to the unloaded hydrogel in the potential range from -0.20 V to 0.60 V. Instead, the moderate variation of the electrochemical activity of PEDOT/Alg(CUR)-h compared to PEDOT/Alg-h is consistent with the preferential interaction between the drug and PEDOT chains. The preferred CUR...PEDOT interaction over CUR...Ca²⁺ one has a clear implication: CUR limits access to the electrically conductive polymer. On the other

hand, the voltammograms recorded for PEDOT/Alg(CUR)-h and Alg(CUR)-h exhibit an increase in current density at around + 0.4 V which corresponds to CUR oxidation. No reduction peak is observed in the scanned potential range because the oxidation of CUR is an irreversible or quasi-irreversible process (depending on the experimental conditions), which agrees with the literature.^{14,54}

The electrochemical stability, represented as the loss of electrochemical activity (LEA; Eq S1) with the number of consecutive oxidation-reduction cycles, is shown in Figure 5b. In all cases the area of the voltammograms and, therefore, the voltammetric charge decreased with the number of cycles, reflecting a loss electrochemical stability. The two PEDOT-containing hydrogels, especially the CUR-loaded one, display the lowest stability. This feature suggests that the interface between the PEDOT and Alg domains becomes seriously affected by the consecutive potential scan cycles. Moreover, this effect is enhanced in PEDOT/Alg(CUR)-h since, apparently, redox processes also affect the PEDOT...CUR interactions, which is expected to be beneficial for the controlled delivery of the drug. It should be noted that the stabilization of the LEA around 20% after 15 redox cycles limits the utilization of PEDOT/Alg-h for applications related with energy storage (e.g. fabrication of electrodes for devices), which require preserving the electrochemical activity for thousands of redox cycles. However, such LEA value does not represent a drawback for the release of drugs in medical applications since in those cases the number of redox cycles needed is relatively low, even for multiple stimulation processes. On the other hand, the structure of Alg-h and Alg(CUR)-h undergoes much fewer changes during the consecutive redox processes, the value of LEA keeping below 10% after 15 cycles.

Non-stimulated release of CUR

A main disadvantage of Ca^{2+} -crosslinked Alg is the low mechanical stability in absence of Ca^{2+} -rich environments, which may affect the drug release rate in biorelevant media by increasing it. Although this drawback can be easily overcome using a number of well-known methods (*e.g.* coating with chitosan, adding selected anions and using an ion diffusion approach during the crosslinking step),^{38,55-57} application of such procedures is out of the scope of this work, which is focused on the preparation, characterization, properties and electrochemical response of PEDOT/Alg-h for drug delivery. Accordingly, in order to avoid distortions in the release results due to the loss of mechanical integrity, a CaCl_2 5% wt. aqueous solution was used as release medium. However, we are aware that stabilization of the hydrogel will be required in a future for *ex vivo* and/or *in vivo* studies

Due to its hydrophobic nature, CUR is poorly soluble in water, even though it is readily soluble in some organic solvents such as ethanol.⁵⁸ PEDOT/Alg(CUR)-h and Alg(CUR)-h square pieces of $1 \times 1 \text{ cm}^2$ were cut and immersed in the aqueous release medium using Eppendorfs. At predefined time intervals (*i.e.* 15 min, 30 min, 1 h, 1 day, 2 days, and 9 days), the release medium (1 mL) was withdrawn from the tube and analyzed by UV-Vis spectroscopy. The amount of released CUR was quantified by UV-vis spectroscopy, using the absorption band centered at 400 nm, and the calibration curve displayed in Figure S2a. More details of the experimental procedure are provided in the Supporting Information.

As shown in Figure 6a, the drug was slowly but progressively released to the medium during the first 1 h. More specifically, $3.6\% \pm 1.0\%$ and $7.1\% \pm 1.0\%$ of CUR from PEDOT/Alg(CUR)-h and Alg(CUR)-h, respectively, was released after this time period. This low release has been attributed to the weak affinity of CUR for water molecules, preferring the interactions with the components of the hydrogels and despite the high SR

observed for the loaded hydrogels. This trend was confirmed after 9 days when the accumulated released drug was kept at practically the same values (*i.e.* $3.3\% \pm 1.0\%$ and $6.9\% \pm 1.0\%$, respectively). In order to accelerate the release, the aqueous medium was substituted by ethanol (99%) at day 9, the corresponding calibration curve is displayed in Figure S2b. After two days, the released CUR increased to $12.9\% \pm 1.7\%$ and $9.1\% \pm 1.4\%$ for PEDOT/Alg(CUR)-h and Alg(CUR)-h, respectively (see a pale yellow rectangle in Figure 6a). However, no additional release was observed after another two days in ethanol. The higher released observed for the PEDOT/Alg(CUR)-h can be explained by the higher SR measured for this hydrogel compared to the Alg(CUR)-h one.

These results indicate that the CUR, a highly hydrophobic drug is not released from the tested hydrogels by a simple diffusion mechanism. In general, the drug release rate depends on (1) drug affinity towards the release medium; (2) desorption of the adsorbed drug from the polymeric molecules, (3) drug diffusion out of the polymeric matrix once desorbed; and (4) the synergy between matrix stimulation and drug diffusion processes. Results displayed in Figure 6a shows that both PEDOT/Alg(CUR)-h and Alg(CUR)-h exhibit small burst and sustained release effects. Considering that the pores of the studied hydrogels are large enough to facilitate the drug diffusion (Figure 3), such effects have been associated not only to the hydrophobicity of CUR but also to the strength of the interactions between the drug and the component of the polymer matrixes, as the results obtained in ethanol demonstrate. In the case of Alg(CUR)-h, the interactions between the drug and Ca^{2+} ions apparently form relatively large hydrophobic complexes, probably with several CUR molecules surrounding each Ca^{2+} ion, causing lower burst effect and slower release than in PEDOT/Alg(CUR)-h. This could explain that the release in ethanol is lower for Alg(CUR)-h than for PEDOT/Alg(CUR)-h, in which CUR molecules presumably interact individually with PEDOT repeat units. This assumption has been

taken as an advantage to explore the CUR release when the PEDOT-containing hydrogel is electrostimulated. Overall, the release profile displayed in Figure 6a reflects that stimuli-assisted drug release devices are necessary to achieve efficient delivery of hydrophobic drugs.

Electrostimulated release of CUR

The electrochemically controlled release of the drug from the hydrogels was carried out in an electrochemical cell filled with 2.5 mL of aqueous solution, as described in the ESI. Electrostimulation was conducted applying an external voltage of either +1.0 V or –1.0 V. The voltage was applied for 2 h interrupted at regular time intervals (every 15 min) for a few minutes to extract the liberation medium for afterward quantification of the released drug, to supplement with fresh liberation medium to keep the volume constant and to record a cyclic voltammogram. The release profiles obtained for PEDOT/Alg(CUR)-h and Alg(CUR)-h using voltages of +1.0 V and –1.0 V are shown in Figures 6b and 6c, respectively; while Figure 7 displays the cyclic voltammograms recorded every 15 min. Figure 8 shows SEM micrographs of the hydrogels after the 2 h electrostimulation and the histograms variation of the pore diameter upon electrostimulation, while the variation of pore area is shown in Figure S3.

The application of a voltage of +1.0 V does not significantly affect the release of CUR from PEDOT/Alg(CUR)-h (Figure 6b). Although the amount of drug released after 15 min of electrostimulation ($7.3\% \pm 2.6\%$) is higher than that achieved by simple diffusion after 1 h ($3.6\% \pm 1.0\%$) (Figure 6a), beyond 15 min the amount of released CUR does not increase with the electrostimulation time, suggesting that PEDOT...CUR interactions are not affected by the application of oxidative potentials. The small difference between the profiles obtained for unstimulated and stimulated with +1.0 V at very short times has been

attributed to the changes induced by the voltage in the structure of the hydrogel, which are discussed below. However, these structural changes are not enough to affect the CUR release at higher times. This interpretation is supported by the cyclic voltammograms recorded at periodic time intervals (Figure 7a), which are all practically identical, reflecting that the hydrogel is not altered by the electrostimulation process. Indeed, the only difference among all of them is a slight decrease in the anodic current, which can be explained by the lesser amount of CUR in the hydrogel because of its release. Also, the CUR oxidation reaction may occur, even though no change in the color of the hydrogel or the release medium was observed. Figure S4 shows the UV spectra of PEDOT/Alg(CUR)-h after the electrical stimuli, the peak is maintained at 400 nm in washed hydrogel even after stimulation at +1.0 V during 2 h, whereas the flat spectrum recorded for unloaded PEDOT/Alg-h (blank) is shown in Figure S5. Although there is an increase in the cross-section pore diameter from $2.6 \pm 0.8 \mu\text{m}$ (for unstimulated hydrogel, Figure 3b) to $6.7 \pm 2.0 \mu\text{m}$ (for +1.0 V stimulated hydrogel (Figure 8c), it seems no affecting significantly the CUR release at +1.0 V. No pores are observed on the surface of the hydrogel. On the other hand, Figure S4 also shows that when CUR is surrounded by an organic environment, the absorbance peak appears at 425 nm

Exposure of Alg(CUR)-h to a potential of +1.0 V for 2 h resulted in a CUR release of $1.9\% \pm 1.4\%$ only (Figure 6b). The latter value, which is reached after only 15 min, is lower than that achieved in absence of stimulus by a factor of 3.6, suggesting that electrostimulation affects the structure of the Alg matrix. The evolution of the cathodic and anodic areas of the voltammograms recorded at periodic time intervals allows us to confirm this hypothesis (Figure 7b). Thus, the electrochemical activity of the hydrogel decreases substantially with increasing time of exposition to the potential until $t = 105$ min. The reduction of the electroactivity is due to the greater difficulties that dopant ions

have in entering into and escaping from the polymer matrix during oxidation and reduction scans, respectively. Thus, the application of the voltage affects the structure of the Alg-h, which becomes more compact, and makes difficult not only the transport of dopant ions but also the delivery of drug molecules. As expected, the average pore diameter of the cross-sectional decreased from 1.9 ± 0.6 to 0.9 ± 0.2 μm after +1.0 V stimulation (Figure 8b). A comparison between the voltammograms displayed in Figure 7a-b indicates that the response of PEDOT/Alg(CUR)-h to chronoamperometric electrostimulation is dominated by the CP domains, even though the Alg domains are expected to be damaged by the applied voltage, like in Alg(CUR)-h.

The release of drug from Alg(CUR)-h increased by $\sim 2\%$ when electrostimulation was performed applying a voltage of -1.0 V (Figure 6c) instead of +1.0 V. Moreover, the release profile obtained for -1.0 V recalls the shape of that achieved in absence of electrostimulation, suggesting that the negative voltage has a lower effect on the porosity of Alg hydrogel than the positive one, even though the diameter of the pores decreased to 1.0 ± 0.3 μm (Figure 8b). This is supported by the cyclic voltammograms displayed in Figure 7d, which show that the reduction of electrochemical activity at increasing electrostimulation time is much less noticeable than in Figure 7b. Also, denoting that Alg hydrogels, in which the electrochemical response is only associated with the diffusion of ions, cannot be employed as electroresponsive drug delivery systems.

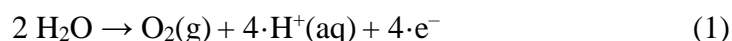
Instead, the electrical stimulation of PEDOT/Alg(CUR)-h, with a sustained application of a voltage of -1.0 V, results in a significant and progressive CUR release (Figure 6c). After only 15 min, the amount of drug found in the release medium is approximately twice and fifteen times higher than those delivered by applying a voltage of +1.0 V (Figure 6b) and simple diffusion (Figure 6a), respectively. Moreover, the release profile reflects a slow but continued release when the negative voltage is applied, reaching a

value of ~25% after 2 h. This represents an increment of ~22% with respect to the non-stimulated delivery achieved after 9 days immersed in an aqueous release medium and of ~19% with respect the stimulated delivery applying a voltage of +1.0 V. The progressive release of CUR is fully consistent with the lower intensity observed in the cyclic voltammograms recorded at intervals of 15 min (Figure 7c). Indeed, the current density in the CV linearly correlates ($R^2= 0.972$) with the amount of CUR released from the hydrogel, as shown in the inset of Figure 6c. On the other hand, the angling of the voltammograms decreases with increasing electrostimulation time, suggesting the electrical contact between PEDOT rich domains increases. This effect can be attributed to released CUR molecules that facilitate the approach of PEDOT chains and/or to the voltage-induced degradation of Alg-rich domains that, despite being lower than for the positive voltage (as discussed above), may be enough to enhance the contact among PEDOT-rich domains. Interestingly, after 2 h electrostimulation, the average pore diameter did not present significant changes (from $2.6 \pm 0.8 \mu\text{m}$ to $2.4 \pm 0.7 \mu\text{m}$), while the surface changed from a smooth to a rugose with pores morphology, which is not observed in any of the other cases and has been attributed to the release of CUR. These suggest that the damage that occurred on the surface of the hydrogel also contributes to CUR release.

The fact that the total amount of released CUR reached only ~25% of the initial dose after 2 h of electrostimulation may be explained by the formation of potential specific interactions between CUR and PEDOT chains (*e.g.* π - π stacking and/or hydrogen bonds). The reduction of the CP by applying a negative electrical voltage probably affects the strength of intermolecular CUR...PEDOT interactions, which become weaker or even cease. This facilitates the release of the drug, even though it is restricted by its

hydrophobic characteristics, which hampers the diffusion of CUR (as observed in Figure 6a).

In addition to the effect of the voltage on the specific interactions and the structure of the hydrogel, the CUR release profiles displayed in Figure 6b-c could be also influenced by other factors, as the change of pH in the hydrogel environment.⁵⁹⁻⁶⁵ More specifically, the production of oxygen and protons due to the oxidation of water molecules when a voltage of + 1.0 V is applied (Eq 1), may cause a pH reduction inside the hydrogel:



Obara *et al.*⁵⁹ reported that, in acidic conditions, the carboxylate groups from Alg chains and the protons bond together, promoting the contraction of the hydrogel due to the neutralization of electrostatic repulsion between the carboxylate groups (Figure 9a). Therefore, the hydrogel becomes more compact, hindering the CUR diffusion.

Instead, water molecules reduce at -1.0 V voltage:



The basic environment caused by the hydroxyl ions favors the deprotonation of carboxylic acid groups from the Alg chain, increasing the amount of negatively charged carboxylate groups and, therefore, the electrostatic repulsion among them (Figure 9a). This favors the swelling of the hydrogel and facilitates the diffusion (Figure 9b). However, it should be emphasized that the poor release profile obtained for Alg(CUR)-h upon the application of -1.0 V (Figure 6c) suggests that, the influence of the pH on the release of the drug from PEDOT/Alg(CUR)-h is very small or even practically null. This feature supports that the influence of the voltage in the structure of the hydrogel and the specific interactions between the drug and polymeric matrix are probably the main driving forces for the release mechanism from such system.

More work needs to be performed to better identify the nature and strength of specific interactions in PEDOT/Alg(CUR)-h, as well as to optimize the release profile. Both the sustained response of the PEDOT/Alg polymeric matrix to the negative voltage and the progressive delivery of CUR support the necessity of future investigations on PEDOT/Alg-h as a promising system for on-demand release. Details about the specific interactions involved in PEDOT/Alg(CUR)-h are expected to be obtained in the near future using computer simulations at the molecular level. Besides, to improve the efficiency of PEDOT/Alg-h as a drug delivery system, future work will focus on optimizing the value of the applied negative voltage and the application of short potential pulse protocols (*i.e.* on/off application of the electrical voltage). Also, investigations using drugs with a less pronounced hydrophobic profile than that of CUR are necessary to alter the balance of the intermolecular interaction. The relative strength between the interactions involving the loaded drug and the molecular species contained in the polymeric matrix and the release medium is a crucial point to regulate the on-demand release. Accordingly, identification of the optimum drug chemical profile for a given polymeric system is necessary to diagnose its effectivity as a drug delivery system.

CONCLUSIONS

PEDOT/Alg hydrogel capable of drug delivery were fabricated. Hydrogels are prepared using a very simple and effective method, which consists of gelling a PEDOT:PSS + AA mixture by adding a CaCl₂ solution. CUR is loaded *in situ* during the gelling process by dissolving the drug with the AA in ethanol before mixing with PEDOT:PSS. Despite PEDOT- and Alg-rich domains are partially segregated, TEM micrographs reveal the presence of conduction paths in the hydrogels, explaining the electroresponsive behavior. Because of both its hydrophobicity and the formation of

intermolecular specific interactions, CUR is slowly released from PEDOT/Alg(CUR) and Alg(CUR) hydrogels by simple diffusion (*i.e.* around 3% only), even when the aqueous release medium is replaced by ethanol. However, the release of drug from PEDOT/Alg(CUR)-h is enhanced in response to electrical stimulation by applying a negative voltage (*i.e.* around 25% in 2 h), which affects intermolecular interactions. Such a stimuli-responsive drug delivery system may find use as drug delivery implants, where the release of the drug can be regulated, according to the patient's requirements through the application of an electrical stimulus.

ASSOCIATED CONTENT

The Supporting Information is available free of charge at <https://pubs.acs.org/doi/>

Experimental methods; GCD curves at different current densities; calibration curves for CUR quantification; histograms displaying the diameter and area of hydrogel pores after applying the electrical stimuli; and UV-Vis spectrum of CUR released after applying the electrical stimuli.

ACKNOWLEDGEMENTS

Authors acknowledge MINECO-FEDER (RTI2018-098951-B-I00) and Agència de Gestió d'Ajuts Universitaris i de Recerca (2017SGR359) for financial support. Support for the research of M.-P.G. and C.A. was received through the prize "ICREA Academia" for excellence in research funded by the Generalitat de Catalunya. J.G.-T. acknowledges the Serra Hunter program of the Generalitat de Catalunya.

REFERENCES

1. Puiggali-Jou, A.; del Valle, L. J.; Alemán, C. Drug Delivery Systems Based on Intrinsically Conducting Polymers. *J. Control. Release* **2019**, *309*, 244–264.
2. Boehler, C.; Oberueber, F.; Asplund M. Tuning Drug Delivery From Conducting Polymer Films for Accurately Controlled Release of Charged Molecules. *J. Control. Release* **2019**, *304*, 1404–1454.
3. Wu, J. G.; Chen, J. H.; Liu, K. T.; Luo, S. C. Engineering Antifouling Conducting Polymers for Modern Biomedical Applications. *ACS Appl. Mater. Interfaces* **2019**, *11*, 21294–21307.
4. Mondal, S.; Das, S.; Nandi, A. K. A Review on Recent Advances in Polymer and Peptide Hydrogels. *Soft Matter* **2020**, *16*, 1404–1454.
5. Tandon, B.; Magaz, A.; Balint, R.; Blaker, J. J.; Cartmell, S. H. Electroactive Biomaterials: Vehicles for Controlled Delivery of Therapeutic Agents for Drug Delivery and Tissue Regeneration. *Adv. Drug Deliv. Rev.* **2018**, *129*, 148–168.
6. Uppalapati, D.; Boyd, B. J.; Garg, S.; Travas-Sejdic, J.; Svirakis, D. Conducting Polymers with Defined Micro- or Nanostructures for Drug Delivery. *Biomaterials* **2016**, *111*, 149–162.
7. Gueye, M. N.; Carella, A.; Faure-Vincent, J.; Demadrille, R.; Simonato, J. P. Progress in Understanding Structure and Transport Properties of PEDOT-Based Materials: A Critical Review. *Prog. Mater. Sci.* **2020**, *108*, 100616.
8. Bubnova, O.; Khan, Z. U.; Wang, H.; Braun, S.; Evans, D. R.; Fabretto, M.; Hojati-Talemi, P.; Dagnelund, D.; Arlin, J. B.; Geerts, Y. H.; Desbief, S.; Breiby, D. W.; Andreasen, J. W.; Lazzaroni, R.; Chen, W. M.; Zozoulenko, I.; Fahlman, M.; Murphy, P. J.; Berggren, M.; Crispin, X. Semi-Metallic Polymers. *Nat. Mater.* **2014**, *13*, 190–194.

9. Kayser, L. V.; Lipomi, D. J. Stretchable Conductive Polymers and Composites Based on PEDOT and PEDOT:PSS. *Adv. Mater.* **2019**, *31*, 1806133.
10. Sappia, L. D.; Piccinini, E.; Marmisolle, W.; Santilli, N.; Maza, E.; Moya, S.; Battaglini, F.; Madrid, R. E.; Azzaroni, O. Integration of Biorecognition Elements on PEDOT Platforms through Supramolecular Interactions. *Adv. Mater. Interf.* **2017**, *17*, 1700502.
11. del Valle, L. J.; Estrany, F.; Armelin, E.; Oliver, R.; Alemán, C. Cellular Adhesion, Proliferation and Viability on Conducting Polymer Substrates. *Macromol Biosci.* **2008**, *8*, 1144–1151.
12. S. C. Luo, E. M. Ali, N. C. Tansil, H. H. Yu, S. Gao, E. A. B. Kantchev, J. Y. Ying. Poly(3,4-ethylenedioxythiophene) (PEDOT) Nanobiointerfaces: Thin, Ultrasoother, and Functionalized PEDOT Films with In Vitro and In Vivo Biocompatibility. *Langmuir* **2008**, *24*, 8071–8077.
13. Puiggali-Jou, A.; del Valle, L. J.; Alemán, C. Drug Delivery Systems Based on Intrinsically Conducting Polymers. *J. Control. Release* **2019**, *309*, 244–264.
14. Puiggali-Jou, A.; Micheletti, P.; Estrany, F.; del Valle, L. J.; Alemán, C. *Electrostimulated Release of Neutral Drugs from Polythiophene Nanoparticles: Smart Regulation of Drug-Polymer Interactions.* *Adv. Healthc. Mater.* **2017**, *6*, 1700453.
15. Puiggali-Jou, A.; del Valle, L. J.; Alemán, C. Encapsulation and Storage of Therapeutic Fibrin-Homing Peptides Using Conducting Polymer Nanoparticles for Programmed Release by Electrical Stimulation. *ACS Biomater. Sci. Eng.* **2020**, *6*, 2135–2145.

16. Esrafilzadeh, D.; Razal, J. M.; Moulton, S. E.; Stewart, E. M.; Wallace, G. G. Multifunctional Conducting Fibres with Electrically Controlled Release of Ciprofloxacin. *J. Control. Release* **2013**, *169*, 313–320.
17. Chen, C.; Chen, X.; Zhang, H.; Zhang, Q.; Wang, L.; Li, C.; Dai, B.; Yang, J.; Liu, J.; Sun, D. Electrically-Responsive Core-Shell Hybrid Microfibers for Controlled Drug Release and Cell Culture. *Acta Biomater.* **2017**, *55*, 434–442,
18. Puiggali-Jou, A.; Cejudo, A.; del Valle, L. J.; Aleman, C. Smart Drug Delivery from Electrospun Fibers Through Electro-Responsive Polymeric Nanoparticles. *ACS Appl. Bio Mater.* **2018**, *1*, 1594–1605.
19. Woepfel, K. M.; Zheng, X. S.; Schulte, Z. M.; Rossi, N. L.; Cui X. Y. T. Nanoparticle Doped PEDOT for Enhanced Electrode Coatings and Drug Delivery. *Adv. Healthc. Mater.* **2019**, *8*, 1900622.
20. Boehler, C.; Oberueber, F.; Asplund, M. Tuning Drug Delivery from Conducting Polymer Films for Accurately Controlled Release of Charged Molecules. *J. Control. Release* **2019**, *304*, 173–180.
21. Carli, S.; Fioravanti, G.; Armirotti, A.; Ciarpella, F.; Prato, M.; Ottonello, G.; Salerno, M.; Scarpellini, A.; Perrone, D.; Marchesi, E.; Ricci, D.; Fadiga, L. A New Drug Delivery System Based on Tauroursodeoxycholic Acid and PEDOT. *Chem. Eur. J* **2019**, *25*, 2322–2329.
22. Krukiewicz, K.; Cinchy, M.; Ruszkowski, P.; Turnzyn, R.; Jarosz, T.; Zak, J. K.; Lapkoski, M.; Bednarczyk-Cwynar; B. Betulin-Loaded PEDOT Films for Regional Chemotherapy. *Mat. Sci. Eng. C Mater.* **2017**, *73*, 611–615.
23. Kleber, C.; Lienkamp, K.; Ruhe, J.; Asplund, M. Electrochemically Controlled Drug Release from a Conducting Polymer Hydrogel (PDMAAp/PEDOT) for Local Therapy and Bioelectronics. *Adv. Healthc. Mater.* **2019**, *8*, 1801488.

24. Molina, B. G.; Dominguez, E.; Armelin, E.; Alemán, C.. Assembly of Conducting Polymer and Biohydrogel for the Release and Real-Time Monitoring of Vitamin K3. *Gels* **2018**, *4*, 86.
25. Xu, Y.; Cui, M.; Patsis, P.; Günter, M.; Yang, X.; Eckert, K.; Zhang, Y. Reversibly Assembled Electroconductive Hydrogel via a Host–Guest Interaction for 3D Cell Culture. *ACS Appl. Mater. Interfaces* **2019**, *11*, 7715–7724.
26. Walker, B. W.; Lara, R. P.; Mogadam, E.; Yu, C. H.; Kimball, W.; Annabi, A. Rational Design of Microfabricated Electroconductive Hydrogels for Biomedical Applications. *Prog. Polym. Sci.* **2019**, *92*, 135–157.
27. Mayr, J.; Diaz Diaz, D. Release of Small Bioactive Molecules from Physical Gels. *Chem. Soc. Rev.* **2018**, *47*, 1484–1515.
28. Culver, H. R.; Clegg, J. R.; Peppas, N. A. Analyte-Responsive Hydrogels: Intelligent Materials for Biosensing and Drug Delivery. *Acc. Chem. Res.* **2017**, *50*, 170–178.
29. Oliva, N.; Conde, J.; Wang, K.; Artzi, N. Designing Hydrogels for On-Demand Therapy. *Acc. Chem. Res.* **2017**, *50*, 669–679
30. Nguyen, M. K.; Alsberg, E. Bioactive Factor Delivery Strategies from Engineered Polymer Hydrogels for Therapeutic Medicine. *Prog. Polym. Sci.* **2014**, *39*, 1235–1265.
31. Vermonden, T.; Censi, R.; Hennink, W. E. Hydrogels for Protein Delivery. *Chem. Rev.* **2012**, *112*, 2853–2888.
32. Li, Y.; Rodrigues, J.; Tomas, H. Injectable and Biodegradable Hydrogels: Gelation, Biodegradation and Biomedical Applications. *Chem. Soc. Rev.* **2012**, *41*, 2193–2221.

33. Chikar, J. A.; Hendricks, J. L.; Richardson-Burns, S. M.; Raphael, Y.; Pflingst, B. E.; Martin, D. C. The Use of a Dual PEDOT and RGD-Functionalized Alginate Hydrogel Coating to Provide Sustained Drug Delivery and Improved Cochlear Implant Function. *Biomaterials* **2012**, *33*, 1982–1990.
34. Marzocchi, M.; Gualandi, I.; Calienni, M.; Zironi, I.; Scavetta, E.; Castellani, G.; Fabroni, B. Physical and Electrochemical Properties of PEDOT:PSS as a Tool for Controlling Cell Growth. *ACS Appl. Mater. Interfaces* **2015**, *7*, 17993–18003.
35. Stritsky, S.; Markova, A.; Vitecek, J.; Safarikova, E.; Hrabal, M.; Kubac, L.; Kubala, L.; Weiter, M.; Vala, M. Printing Inks of Electroactive Polymer PEDOT:PSS: The Study of Biocompatibility, Stability, and Electrical Properties. *J. Biomed. Mater. Res. A* **2018**, *106*, 1121–1128.
36. Heo, D. N.; Lee, S. J.; Timsina, R.; Qiu, X. Y.; Castro, N. J.; Zhang, L. G. Development of 3D Printable Conductive Hydrogel with Crystallized PEDOT:PSS for Neural Tissue Engineering. *Mat. Sci. Eng. C Mater.* **2019**, *99*, 582–590.
37. Guex, A. G.; Puetzer, J. L.; Armgarth, A.; Littmann, E.; Stavrinidou, E.; Giannelis, E. P.; Malliaras, G. G.; Stevens, M. M. Highly Porous Scaffolds of PEDOT:PSS for Bone Tissue Engineering. *Acta Biomater.* **2017**, *62*, 91–101.
38. Lee, K. Y.; Mooney, D. J. Alginate: Properties and Biomedical Applications. *Prog. Polym. Sci.* **2012**, *37*, 106–26.
39. Reakasame, S.; Boccaccini, A. R. Oxidized Alginate Based Hydrogels for Tissue Engineering Applications: A Review. *Biomacromolecules* **2018**, *19*, 3–21.
40. Szekalska, M.; Puciłowska, A.; Szymańska, E.; Ciosek, P.; Winnicka, K. Alginate: Current Use and Future Perspectives in Pharmaceutical and Biomedical Applications. *Int. J. Polym. Sci.* **2016**, *2016*, 1–17.

41. Anand, P.; Kunnumakkara, A. B.; Newman, R. A.; Aggarwal, B. B. Bioavailability of Curcumin: Problems and Promises. *Mol. Pharm.* **2007**, *4*: 807–818.
42. Mahady, G. B.; Pendland, S. L.; Yun, G.; Lu, Z. Z. Turmeric (*Curcuma longa*) and Curcumin Inhibit the Growth of *Helicobacter Pylori*, a Group 1 Carcinogen. *Anticancer Res.* **2002**, *22*, 4179–4181.
43. Reddy, R. C.; Vatsala, P. G.; Keshamouni, V. G.; Padmanaban, G.; Rangarajan, P. N. Curcumin for Malaria Therapy. *Biochem. Biophys. Res. Commun.* **2005**, *326*, 472–474.
44. Venkatesan N.; Punithavathi, D.; Arumugam, V. Curcumin Prevents Adriamycin Nephrotoxicity in Rats. *Br. J. Pharmacol.* **2000**, *129*, 231–234.
45. Arun, N.; Nalini, N. Efficacy of Turmeric on Blood Sugar and Polyol Pathway in Diabetic Albino Rats. *Plant. Foods Hum. Nutr.* **2002**, *57*, 41–52.
46. Pérez-Madrugal, M. M.; Torras, J.; Casanovas, J.; Häring, M.; Alemán, C.; Díaz, D. Paradigm Shift for Preparing Versatile M²⁺-Free Gels from Unmodified Sodium Alginate. *Biomacromolecules* **2017**, *18*, 2967–2979.
47. Plazinski, W.; Drach, M. Calcium- α -1-Guluronate Complexes: Ca^{2+} Binding Modes from DFT-MD Simulations. *J. Phys. Chem. B* **2013**, *117*, 12105–12112.
48. Yang, C.; Tibbitt, M. W.; Basta, L.; Anseth, K. S. Mechanical Memory and Dosing Influence Stem Cell Fate. *Nat. Mater.* **2014**, *13*, 645–652.
49. Ma, Y.; Lin, M.; Huang, G.; Li, Y.; Wang, S.; Bai, G.; Lu, T. J.; Xu, F. 3D Spatiotemporal Mechanical Microenvironment: A Hydrogel-Based Platform for Guiding Stem Cell Fate. *Adv. Mater.* **2018**, *30*, 1–27.
50. Guimarães, C. F.; Gasperini, L.; Marques, A. P.; Reis, R. L. The Stiffness of Living Tissues and Its Implications for Tissue Engineering. *Nat. Rev. Mater.* **2020**, *5*, 351–370 (2020).

51. Pailler-Mattei, C.; Bec, S.; Zahouani, H. In Vivo Measurements of the Elastic Mechanical Properties of Human Skin by Indentation Tests. *Med. Eng. Phys.* **2008**, *30*, 599–606.
52. Rho, J. Y.; Ashman, R. B.; Turner, C. H. Young's Modulus of Trabecular and Cortical Bone Material: Ultrasonic and Microtensile Measurements. *J. Biomech.* **1993**, *26*, 111–119.
53. Li, X.; Wei, B. Facile Synthesis and Super Capacitive Behavior of SWNT/MnO₂ Hybrid Films. *Nano Energy* **2012**, *1*, 479–487.
54. Masek, A.; Chrzescijanska, E.; Zaborski, M. Characteristics of Curcumin Using Cyclic Voltammetry, UV–Vis, Fluorescence and Thermogravimetric Analysis. *Electrochim. Acta* **2013**, *107*, 441–447.
55. Bajpai, M.; Shukla, P.; Bajpai, S. K. Enhancement in the Stability of Alginate Gels Prepared with Mixed Solution of Divalent Ions Using a Diffusion Through Dialysis Tube (DTDT) Approach. *J. Macromol. Sci., Part A* **2017**, *54*, 301–310.
56. Matricardi, P.; di Meo, C.; Coviello, T.; Alhaique, F. Recent Advances and Perspectives on coated Alginate Microspheres for Modified Drug Delivery. *Expert Opin. Drug Del.* **2008**, *5*, 417–425.
57. Abasalizadeh, F.; Moghaddam, S. V.; Alizadeh, E.; Akbari, E.; Kashani, E.; Fazljou, S.; Torbati, M.; Akbarzadeh, A. Alginate-Based Hydrogels as Drug Delivery Vehicles in Cancer Treatment and Their Applications in Wound Dressing and 3D Bioprinting. *J. Biol. Eng.* **2020**, *14*, 8.
58. Priyadarsini, K. I. Photophysics Photochemistry and Photobiology of Curcumin. Studies from Organic Solutions Bio-mimetics and Living Cells. *J. Photochem. Photobiol. C* **2009**, *10*, 81–95.

59. Obara, S.; Yamauchi, T.; Tsubokawa, N. Evaluation of the Stimulus Response of Hydroxyapatite/ Calcium Alginate Composite gels. *Polym. J.* **2010**, *42*, 161–166.
60. Shi, X.; Zheng, Y.; Wang, C.; Yue, L.; Qiao, K.; Wang, G.; Wang, L.; Quan, H. Dual Stimulus Responsive Drug Release Under the Interaction of pH Value and Pulsatile Electric Field for a Bacterial Cellulose/Sodium Alginate/Multi-Walled Carbon Nanotube Hybrid Hydrogel. *RSC Adv.* **2015**, *5*, 41820–41829.
61. Shi, X., Zheng, Y., Wang, G., Lin, Q.; Fan, J. Ph- and Electro-Response Characteristics of Bacterial Cellulose Nanofiber/Sodium Alginate Hybrid Hydrogels for Dual Controlled Drug Delivery. *RSC Adv.* **2014**, *4*, 47056–47065.
62. Abd El-Ghaffar, M. A.; Hashem, M. S.; El-Awady, M. K.; Rabie, A. M. Ph-Sensitive Sodium Alginate Hydrogels for Riboflavin Controlled Release. *Carbohydr. Polym.* **2012**, *89*, 667–675.
63. Lima, D. S.; Tenório-Neto, E. T.; Lima-Tenório, M. K.; Guiherme, M. R.; Scariot, D. B.; Nakamura, C. V.; Muniz, E. C.; Rubira, A. F. pH-Responsive Alginate-Based Hydrogels for Protein Delivery. *J. Mol. Liq.* **2018**, *262*, 29–36.
64. Ben Messaoud, G.; Sánchez-González, L.; Probst, L.; Jeandel, C.; Arab-Tehrany, E.; Desobry, S. Physico-Chemical Properties of Alginate/Shellac Aqueous-Core Capsules: Influence of Membrane Architecture on Riboflavin Release. *Carbohydr. Polym.* **2016**, *144*, 428–437.
65. Nayak, A. K.; Pal, D. Development of pH-Sensitive Tamarind Seed Polysaccharide-Alginate Composite Beads for Controlled Diclofenac Sodium Delivery Using Response Surface Methodology. *Int. J. Biol. Macromol.* **2011**, *49*, 784–793.

CAPTIONS TO FIGURES

Figure 1. (a) Sketch illustrating the procedure used to prepare PEDOT/Alg(CUR)-h: (1) equal volumes of PEDOT:PSS aqueous dispersion and AA solution in water:ethanol were mixed; (2) 0.7 mL of the PEDOT:PSS + AA mixture were deposited on a ITO sheet, which was subsequently sandwiched between two cover glasses separated by plastic strips; (3) the sandwiched ITO sheet was placed in a petri dish that was subsequently filled with a CaCl₂ solution; and (4) the formed hydrogels were extracted and washed after 24 h. (b) Photographs of the prepared hydrogels just after the gelling step. (c) FTIR spectra and (d) swelling ratio of the prepared hydrogels.

Figure 2. (a) Cell adhesion (24 h) and (b) cell proliferation (7 days) of Hff and MG-63 cells on Alg-h and PEDOT/Alg-h. The relative viabilities were established in relation to tissue culture polystyrene (TCPS), which was considered as a control substrate. Asterisk mark represents a significant difference among the other samples at $p < 0.05$ (*) and $p < 0.001$ (***)).

Figure 3. (a) Cross-sectional (low and high magnification at top and bottom, respectively) and surface (low and high magnification at top and bottom, respectively) SEM micrographs of: Alg-h; PEDOT/Alg-h; Alg(CUR)-h and PEDOT/Alg(CUR)-h. Bars in high and low-resolution micrographs: 500 nm and 5 μ m, respectively. Histograms displaying (b) the diameter and (c) area of the pores observed in the cross-sections

Figure 4. (a) TEM micrographs with different magnifications (from low at the left to high at the right and bottom) of the same region of stained PEDOT/Alg-h. (b) TEM micrographs of unstained PEDOT/Alg-h.

Figure 5. For PEDOT/Alg(CUR)-h, PEDOT/Alg-h, Alg(CUR)-h and Alg-h: (a) Cyclic voltammograms recorded from -0.20 to 0.60 V at a scan rate of 100 mV/s; and (b)

Variation of the loss of electrochemical activity (LEA) against the number of consecutive redox cycles.

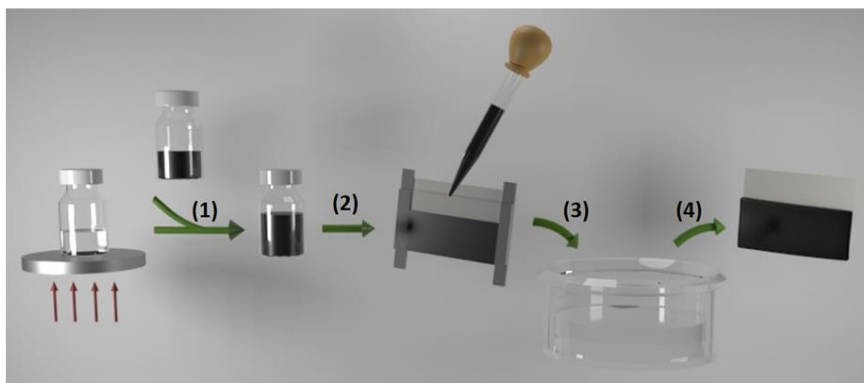
Figure 6. CUR release from PEDOT/Alg(CUR)-h and Alg(CUR)-h samples by (a) diffusion (passive release) after immersion in an aqueous solution for 9 days and ethanol (pale yellow rectangle) for four days, and by applying a constant potential of (b) +1.0 V or (c) -1.0 V for 2 h in aqueous solution. The inset in (c) shows the correlation between the current density (from cyclic voltammograms) and the amount of CUR released from the hydrogel.

Figure 7. Cyclic voltammograms recorded at 15 min intervals for (a, c) PEDOT/Alg(CUR)-h and (b, d) Alg(CUR)-h electrostimulated by applying a constant voltage of (a, b) +1.0 V or (c, d) -1.0 V. All voltammograms were obtained in the potential window comprised between -0.20 and 0.60 V at a scan rate of 100 mV/s.

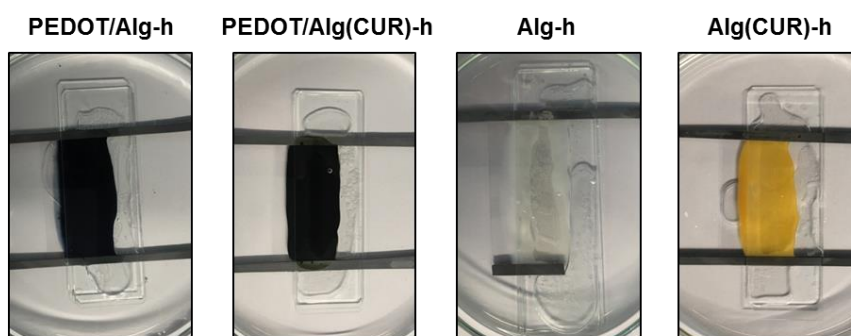
Figure 8. (a) Cross-sectional (low and high magnification at top and bottom, respectively) and surface (low and high magnification at top and bottom, respectively) SEM micrographs of Alg(CUR)-h and PEDOT/Alg(CUR)-h after undergoing -1.0 or +1 V electrostimulation (left and right, respectively). Bars in high and low-resolution micrographs: 500 nm and 5 μ m, respectively. Histogram representing the diameter of the pores found on the cross-sectional profiles in (b) Alg(CUR)-h and (c) PEDOT/Alg(CUR)-h before (Ctrl) and after applying the electrical stimuli.

Figure 9. (a) Effect of pH and electrical stimuli on the Alg chain. (b) Scheme of PEDOT/Alg(CUR)-h hydrogel changes after undergoing - 1.0 V electrostimulation.

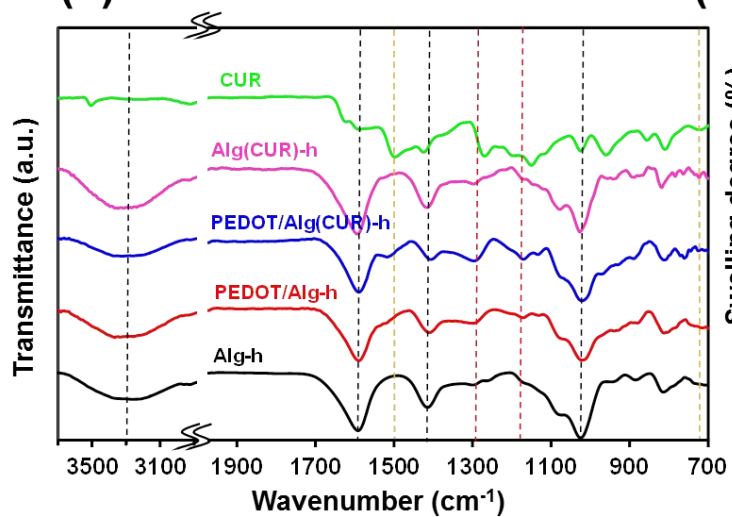
(a)



(b)



(c)



(d)

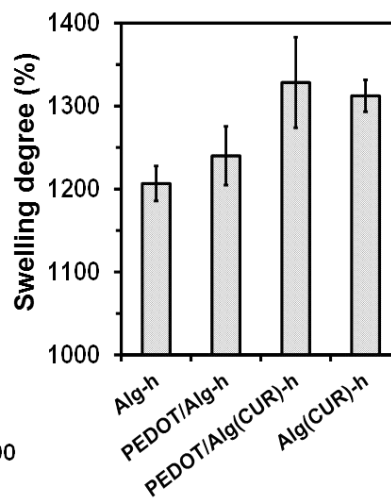


Figure 1

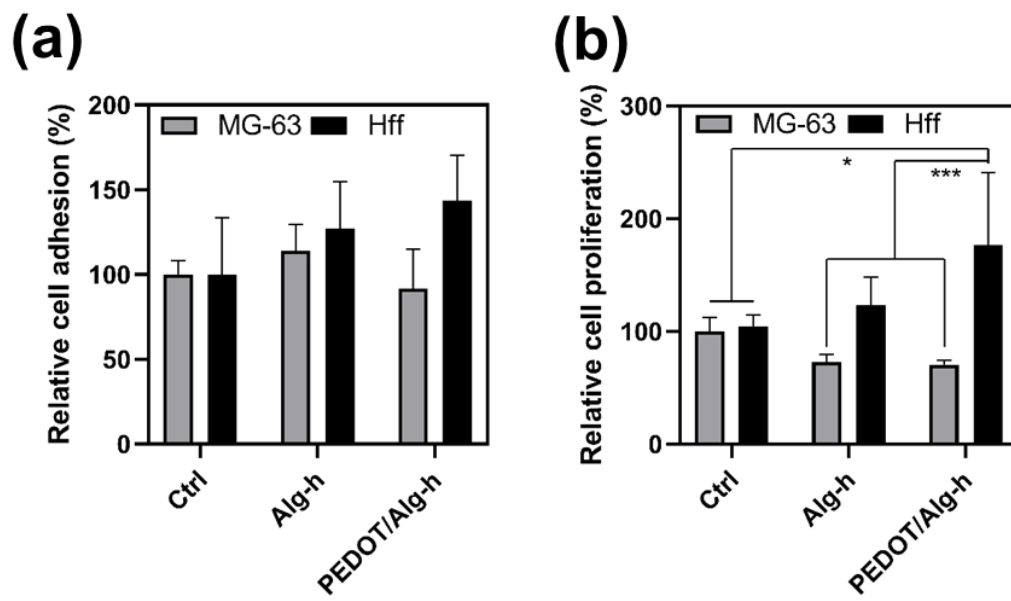


Figure 2

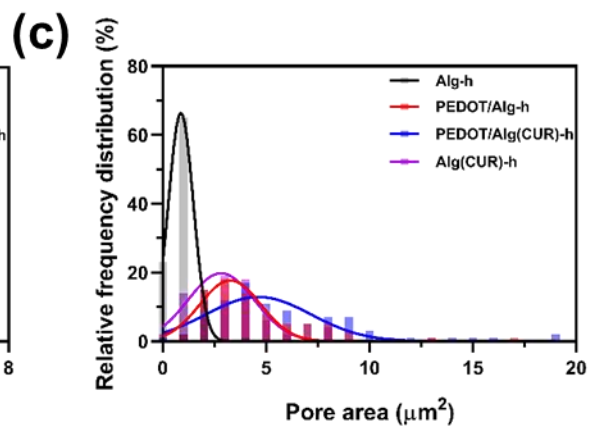
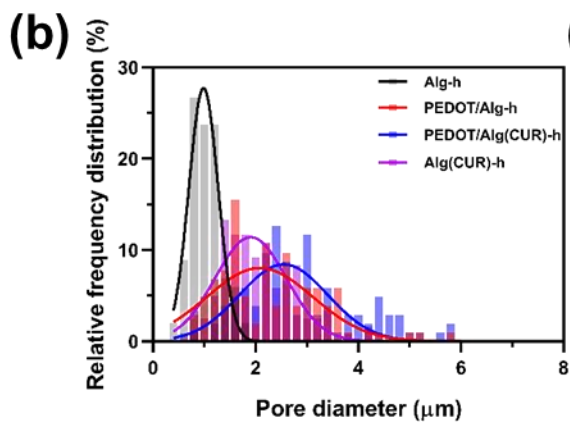
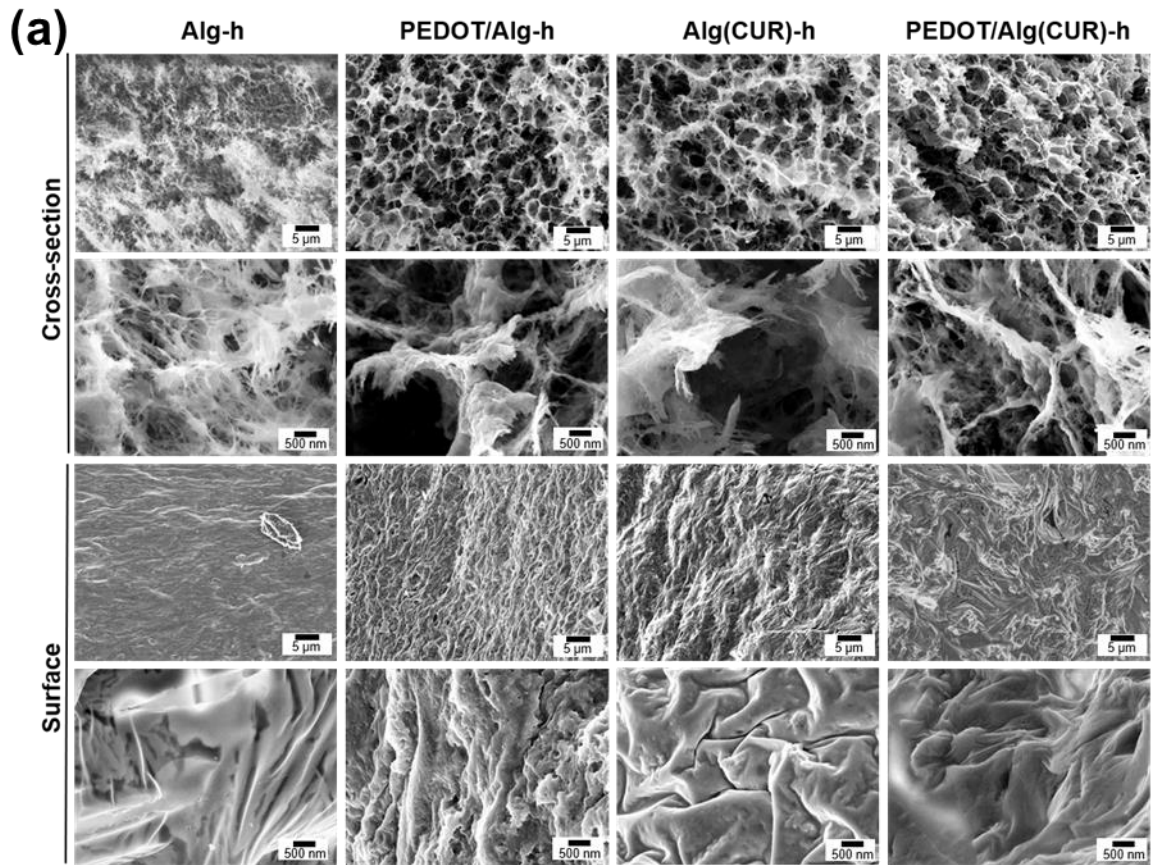
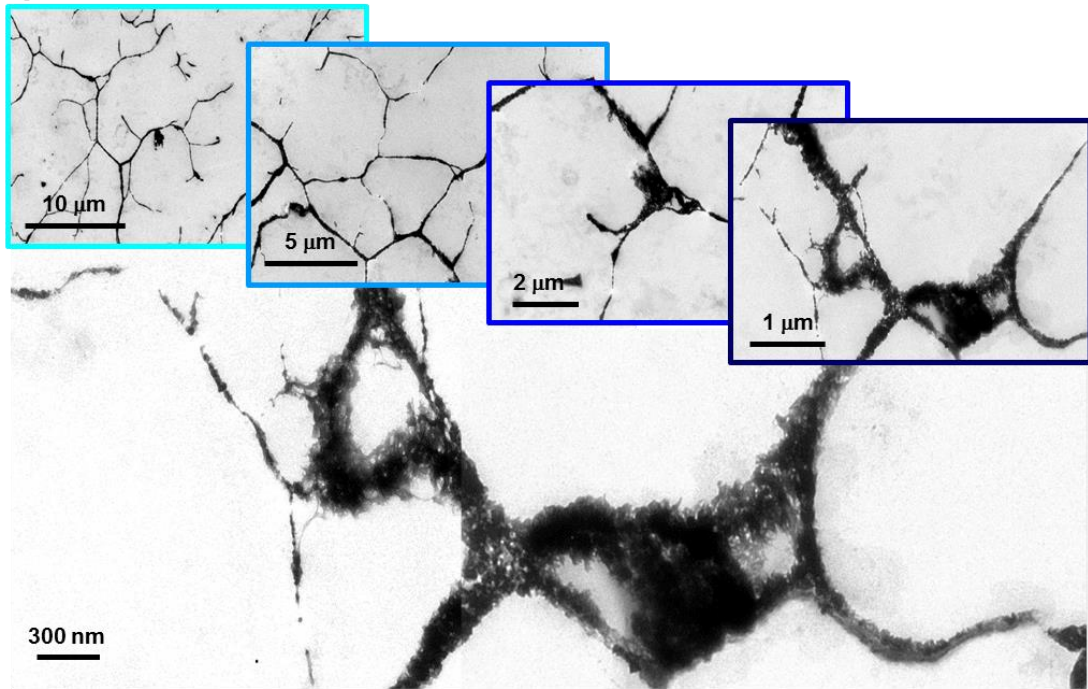


Figure 3

(a)



(b)

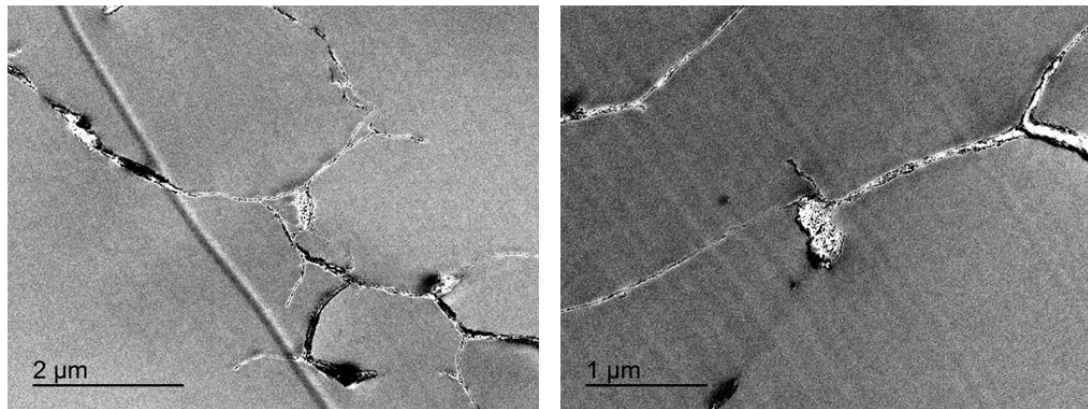


Figure 4

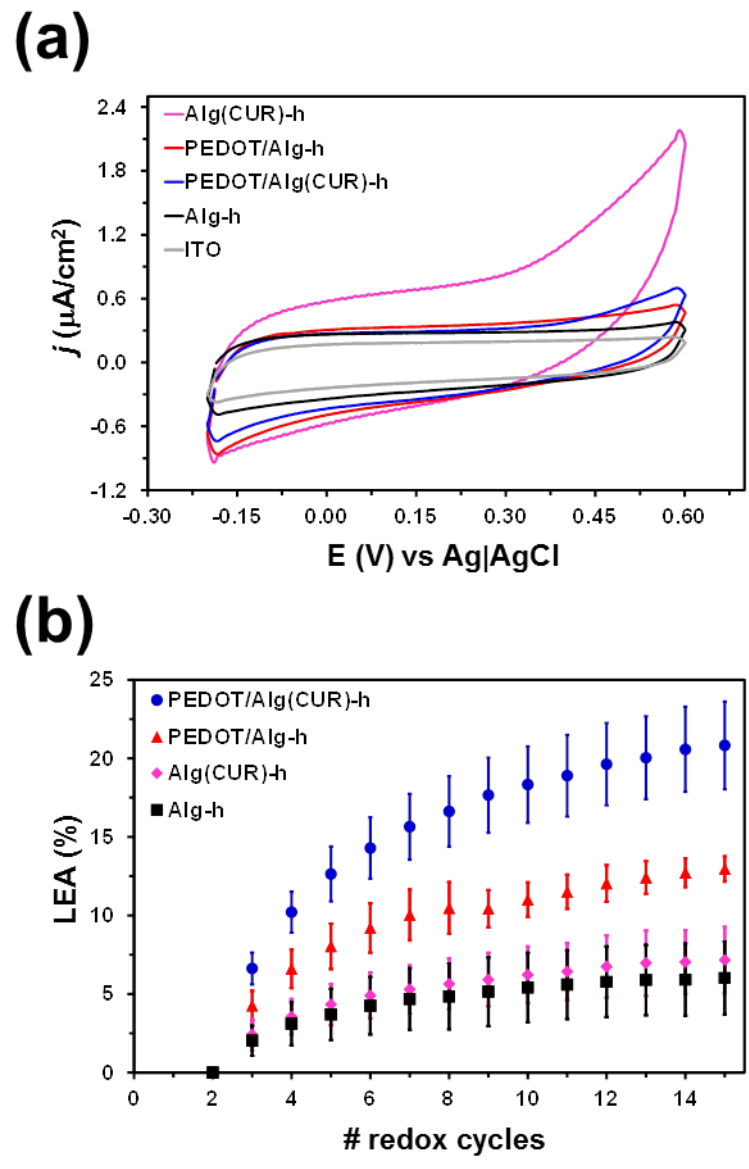


Figure 5

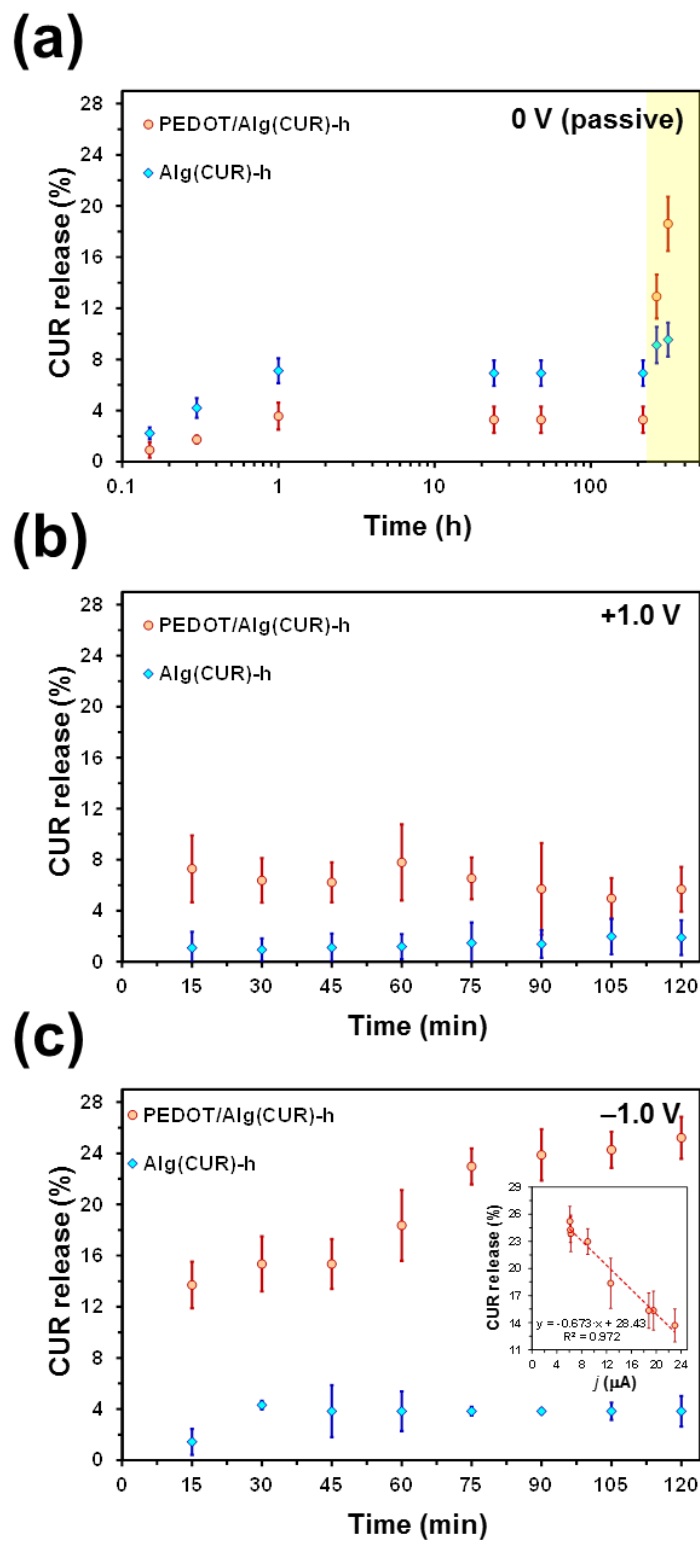


Figure 6

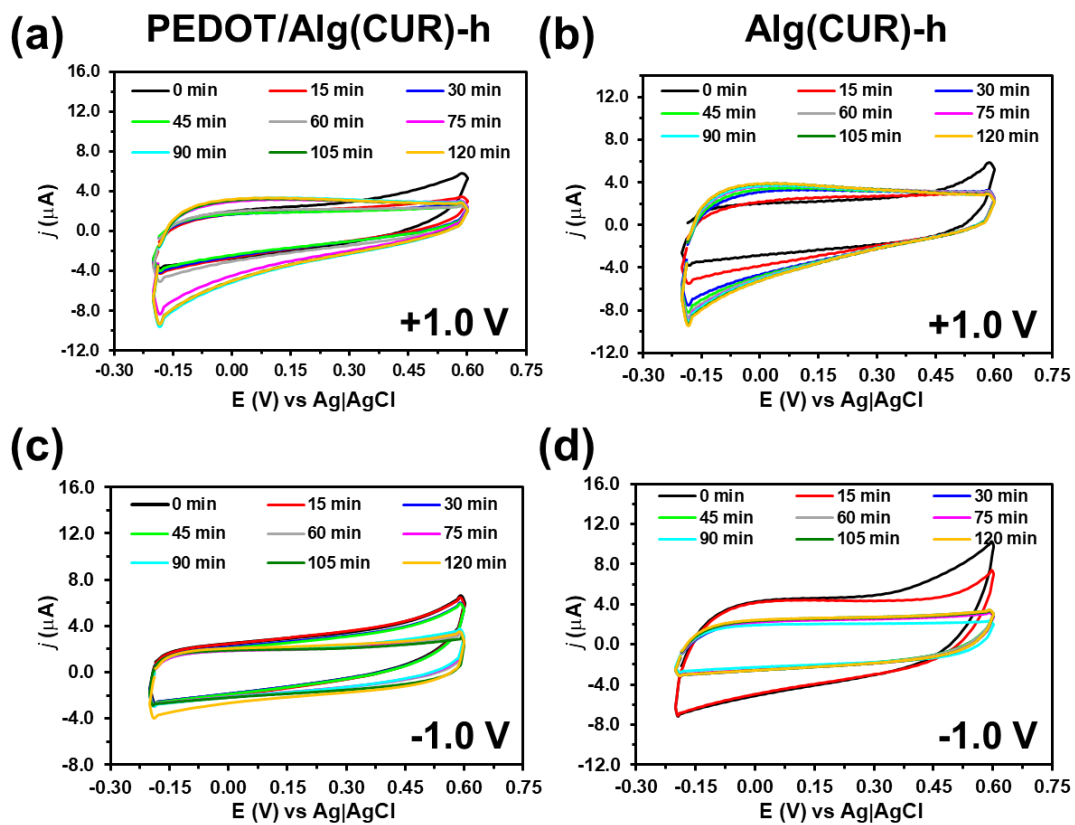


Figure 7

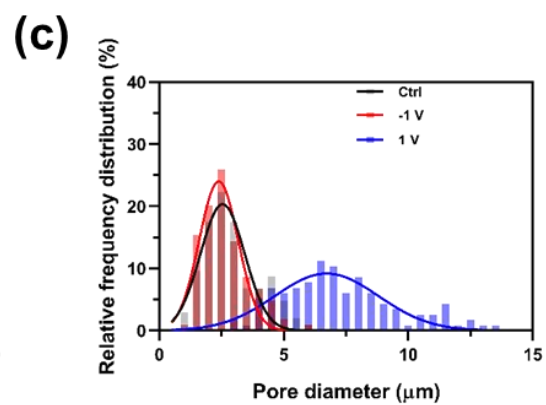
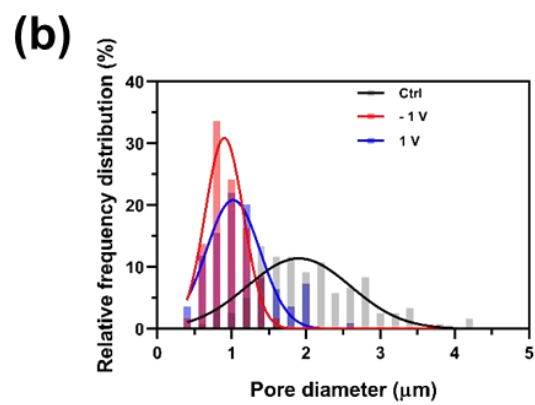
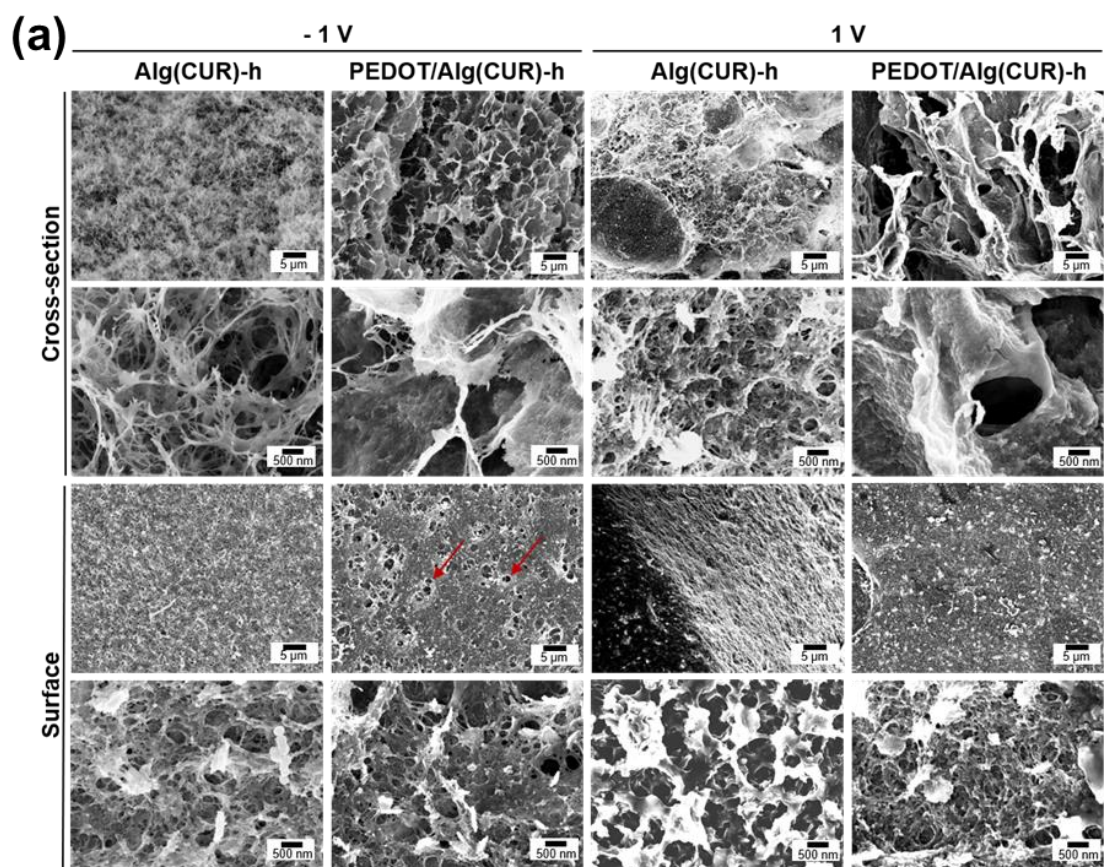


Figure 8

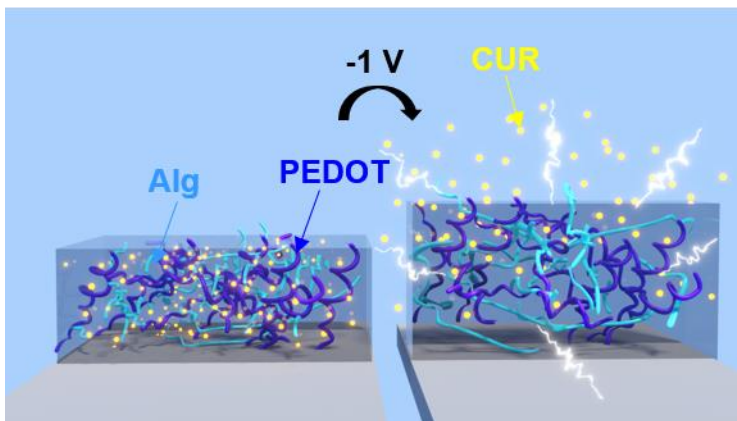
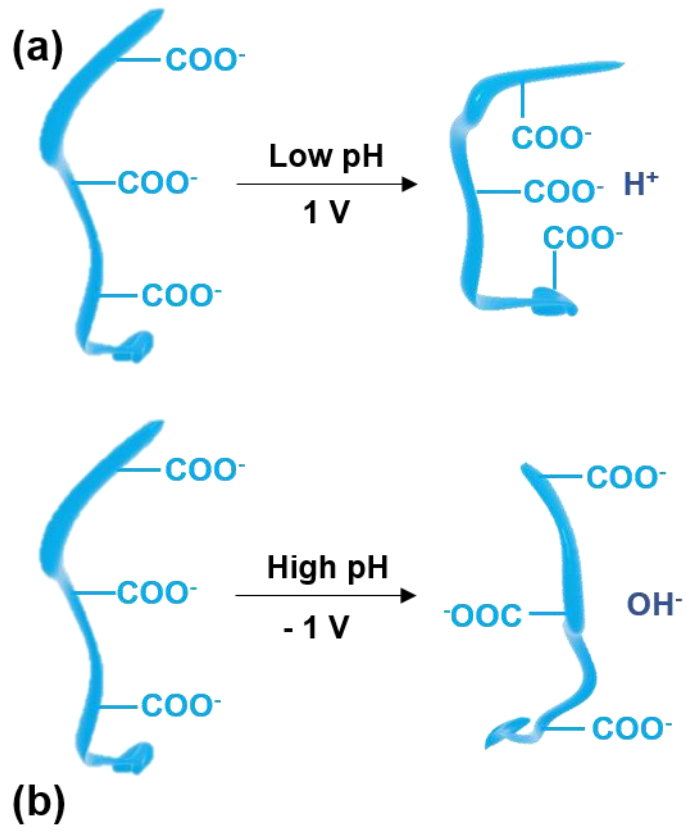


Figure 9